aquaculture journal

MDPI

Article

Prediction of Shrimp Growth by Machine Learning: The Use of Actual Data of Industrial-Scale Outdoor White Shrimp (*Litopenaeus vannamei*) Aquaculture in Indonesia

Muhammad Abdul Aziz Al Mujahid [1], Fahma Fiqhiyyah Nur Azizah [1], Gun Gun Indrayana [2], Nina Rachminiwati [2], Yutaro Sakai [1] and Nobuyuki Yagi [1,*]

[1] Graduate School of Agricultural and Life Sciences, The University of Tokyo, 1-1-1 Yayoi, Bunkyo, Tokyo 113-8657, Japan
[2] PT. Inovasi Akuakultur Muda, Graha Kompas Gramedia, Jl. LLRE Martadinata no 46, Bandung 40115, Indonesia
* Correspondence: yagi@g.ecc.u-tokyo.ac.jp; Tel.: +81-3-5841-5599

Abstract

Accurate prediction of shrimp body weight is critical for optimizing harvest timing, feed management, and stocking density decisions in intensive aquaculture. While prior studies emphasize environmental factors, operational management variables—particularly harvesting metrics—remain understudied. This study quantified the predictive importance of harvesting-related variables using 5 years of industrial-scale operational data from 12 ponds (5479 cleaned records, 34.94% retention rate). We trained seven machine learning models and applied three independent feature importance methods: consensus importance ranking, SHAP explainability analysis, and Pearson correlations. Main findings: Operational variables (days of culture: 2.833 SHAP, stocking density: 1.871, cumulative feed: 1.510) ranked substantially above environmental variables (temperature: 0.123, pH: 0.065, dissolved oxygen: 0.077). Partial harvest frequency showed bimodal clustering, indicating two distinct viable operational strategies. The Weighted Ensemble model achieved the highest performance (R^2 = 0.829, RMSE = 4.23 g, MAE = 3.12 g). Model stability analysis via 10-fold GroupKFold cross-validation showed that the Artificial Neural Network (ANN) exhibited the tightest confidence bounds (0.708 g width, 27.7% coefficient of variation), indicating exceptional consistency. This is the first study to systematically analyze the importance of harvesting variables using SHAP explainability, revealing that operational management decisions may yield greater returns than marginal environmental control investments. Our findings suggest that operational optimization may be more impactful than environmental fine-tuning in well-managed systems.

Keywords: aquaculture; machine learning; SHAP explainability; operational management; harvesting strategy; feature importance

check for updates

Academic Editor: Aires Oliva-Teles

Received: 16 October 2025
Revised: 2 December 2025
Accepted: 2 December 2025
Published: 5 December 2025

Citation: Mujahid, M.A.A.A.; Azizah, F.F.N.; Indrayana, G.G.; Rachminiwati, N.; Sakai, Y.; Yagi, N. Prediction of Shrimp Growth by Machine Learning: The Use of Actual Data of Industrial-Scale Outdoor White Shrimp (*Litopenaeus vannamei*) Aquaculture in Indonesia. *Aquac. J.* **2025**, *5*, 27. https://doi.org/10.3390/aquacj5040027

Copyright: © 2025 by the authors. Licensee MDPI, Basel, Switzerland. This article is an open access article distributed under the terms and conditions of the Creative Commons Attribution (CC BY) license (https://creativecommons.org/licenses/by/4.0/).

1. Introduction

1.1. Background

Aquaculture production reached 130.9 million tonnes in 2022 and continues growing at 5–7% per year, contributing substantially to global food security [1]. The global shrimp market is projected to grow from USD 70.09 billion in 2025 to USD 151.32 billion by 2035, at a CAGR of 8.0%, driven by rising consumer preference for seafood and technological

advances in aquaculture [2]. White shrimp (*Litopenaeus vannamei*) accounts for approximately 80% of global farmed shrimp production, totaling ~4.4 million metric tons annually, and serves as a critical protein source in Southeast Asia and Latin America, supporting approximately 2.5 million direct jobs globally [3].

Intensive farming faces critical challenges: disease outbreaks cause >30% production losses in some facilities [4,5], while high stocking densities reduce individual growth rates and increase stress-related mortality [6]. Feed costs account for 40–60% of total production expenses [7], yet recent AI applications demonstrate that machine learning-based innovative feeding systems can improve feed conversion ratios by up to 30% and reduce waste [8]. Accurate growth prediction enables optimizing stocking density, predicting harvest timing, and adjusting feeding rates—critical objectives for both productivity and sustainability [9,10].

1.2. Research Gap: Environmental Focus vs. Operational Variables

The classical aquaculture literature emphasizes water quality as the primary determinant of growth. Previous studies have identified dissolved oxygen, temperature, pH, and salinity as critical environmental factors [11,12]. Machine learning applications in aquaculture have similarly focused on environmental parameters [13], yet recent reviews highlight that predictive AI systems for disease detection and health monitoring can reduce mortality by 20%, suggesting that operational factors warrant equal attention [14,15].

While partial harvesting is an established commercial operational practice in intensive aquaculture, few predictive models have integrated harvesting strategy variables, which represents a significant research opportunity to optimize this ubiquitous management practice [16]. While previous work has examined the economic benefits of partial harvesting (4.3% revenue improvement potential), demonstrating that well-designed harvesting schemes enhance aquaculture profitability, no prior study has systematically quantified the predictive importance of harvesting variables using explainable machine learning methods. Recent applications of SHAP and interpretable ML in aquaculture demonstrate high predictive accuracy (98.99% for management decisions, 96–97% for disease detection) but have focused primarily on environmental parameters and price prediction; applying similar explainable methods to harvesting strategy optimization represents a significant research gap [16–18].

The critical question: In industrial aquaculture with tight environmental control, what is the relative importance of operational variables versus environmental parameters in predicting individual growth?

1.3. Machine Learning and Explainability Approaches

Machine learning offers significant advantages for predicting complex outcomes in aquaculture by capturing nonlinear relationships and feature interactions that traditional statistical methods cannot model. Aquaculture data affected by complex environmental factors are typically nonlinear and multidimensional; traditional regression approaches fail to capture synergistic and antagonistic interactions among variables. In contrast, deep learning models automatically extract hierarchical features. They can model nonlinear relationships via combinations of functions, achieving substantially higher accuracy (e.g., 98.64% for fish classification, 96% R^2 for production forecasting) than traditional nonlinear regression approaches. Ensemble-based algorithms (XGBoost, Random Forest) and neural networks demonstrate particular superiority in modeling complex water quality interactions critical to growth prediction [19–21]. Recent applications demonstrate that AI-powered predictive analytics can flag potential disease threats, such as White Spot Syndrome Virus (WSSV) and Early Mortality Syndrome (EMS), before symptoms appear, enabling proactive interventions. Machine learning models achieve 97–100% accuracy in early WSSV detection, while LSTM-based water quality prediction systems provide 24–48 h warning of disease-conducive conditions, allowing

farmers to implement preventive measures before mortality escalates [15,22–24]. The field of artificial intelligence in aquaculture is experiencing rapid market expansion and institutional adoption, with research indicating significant growth in AI-powered precision farming systems, innovative feeding technologies, and disease monitoring platforms. Industry analysis documents emerging applications in biomass estimation, automated feeding optimization, and early disease warning systems, driving adoption across Southeast Asia, Latin America, and North America [25,26].

While machine learning models excel at prediction, their mechanistic interpretability has been limited. SHAP (SHapley Additive exPlanations) is a mathematically rigorous framework for quantifying feature contributions to predictions, unifying disparate interpretability methods under a single theoretical foundation grounded in game theory. SHAP assigns each feature an importance value for a particular prediction by computing Shapley values across all possible feature coalitions, providing both local explanations (for individual predictions) and global explanations (for model-level patterns) [27–30]. Recent applications demonstrate SHAP's effectiveness in identifying critical factors across multiple agricultural domains. In food engineering, SHAP provides transparent identification of factors that determine food quality, safety, and authenticity, enabling tasks such as contaminant detection and nutritional value estimation using spectral and imaging data. In crop yield prediction, SHAP analysis quantifies the spatial and temporal drivers of production with median linear correlation coefficients of 0.67, identifying production volume, area, and fertilizer application as primary contributors to yield variability. In animal production, SHAP-based explainable machine learning models monitor dairy cattle health and activity patterns through accelerometer data, enabling the early detection of behavioral changes indicative of illness or stress before clinical symptoms manifest [31–34].

1.4. Study Objectives and Hypotheses

This study quantifies the importance of operational versus environmental variables for shrimp growth prediction using five years of commercial-scale operational data from 12 ponds (5479 cleaned records), employing seven machine learning models and three independent feature importance methods (consensus importance, SHAP explainability, and Pearson correlations).

Objectives:

- Quantify the relative importance of operational management versus environmental variables in predicting shrimp mean body weight.
- Develop an efficient growth-prediction model for real-time farm decision-support systems.
- Provide statistical validation through 10-fold GroupKFold cross-validation and 95% confidence intervals.

Hypotheses:

- Operational Primacy: Operational variables (days of culture, stocking density, feeding, harvesting) rank higher than environmental variables in production environments with tight environmental control.
- Partial Harvesting Significance: Partial harvesting variables constitute major predictors of individual growth.
- Ensemble Efficiency: Ensemble methods achieve performance equivalent to deep learning models with reduced computational requirements.

1.5. Innovation and Contribution

This is the first systematic study to incorporate partial-harvesting variables as primary predictors in aquaculture growth models, using SHAP explainability analysis. Unlike

prior work that emphasizes environmental factors such as water quality (dissolved oxygen, temperature, pH, salinity) as dominant determinants of growth, our analysis quantifies the predictive power of harvesting metrics—revealing that operational management decisions may yield greater returns than marginal improvements in environmental control [35,36]. Advanced regression models, including Random Forest, LightGBM, and hybrid LSTM-RF architectures, when combined with SHAP and LIME explainability frameworks, enable transparent identification of feature interactions and critical factors across diverse agricultural domains [29]. This work represents a paradigm shift from traditional environmental monitoring to operational management recognition, with direct implications for farm-level decision-support systems and sustainable aquaculture practices.

2. Materials and Methods

2.1. Study Facility

2.1.1. Software Framework and Computational Environment

All analyses were conducted using Python 3.9 on a local Mac mini M4 (16 GB RAM) with standard scientific libraries (scikit-learn 1.6.1, PyTorch 2.8.0, SHAP 0.49.1). Ten-fold cross-validation (80 iterations per model) was executed with parallelization via scikit-learn's n_jobs parameter. ANN training used PyTorch's CPU backend. SHAP analysis (200 samples per feature) employed KernelExplainer with parallel batch processing. All random seeds were explicitly set (random_state = 42) for reproducibility. The complete pipeline required approximately 10 h of computation.

2.1.2. Study Facility and Description

The study was conducted at an industrial-scale aquaculture facility in West Java, Indonesia, specializing in the production of white shrimp (*Litopenaeus vannamei*). The facility operates 12 outdoor earthen ponds, each approximately 1.5 hectares in area and with an average depth of 1.2 m. The facility employs intensive management practices, including mechanical aeration, daily feeding protocols, and routine water quality monitoring. Data were collected during 14 consecutive production cycles spanning 2017–2022 (5 years).

2.2. Data Sources and Preprocessing

2.2.1. Raw Dataset Characteristics

Production records were compiled from the facility's operational database, using standardized data-collection protocols. Raw data contained 15,683 daily records across all ponds and cycles with the following features: Day of Cultivation (30–130 days), Mean Body Weight (grams), Daily Feeding Amount (kilograms), Cumulative Feeding (kilograms), Partial Harvest Count (number of events), Cumulative Harvest Mass (kilograms), Individual Harvest Mass (kilograms), Pond Size (square-meter), Stocking Density (number of individuals per square meter), Number of Aerators (count), Water Temperature (°C), Dissolved Oxygen (mg/L), pH (unitless), Salinity (ppt), and Alkalinity (mg/L $CaCO_3$). A summary of the data is represented in Table 1.

Table 1. Shrimp farming parameters found in the dataset. This study utilized real production data from a super-intensive outdoor shrimp aquaculture. The data is divided into several categories: temporal, infrastructure, operational, and environmental.

Category	Parameter	Description
Target	Mean body weight	Mean body weight of shrimp
Temporal	Day of cultivation	Rearing period since the introduction of post-larvae to the ponds

Table 1. *Cont.*

Category	Parameter	Description
Pond (Infrastructure)	Stocking density	Initial number of shrimps in a pond
	Pond size	Pond area in meter square
	Aerator count	Number of active aerators in a pond
Feeding (Operational)	Feeding amount	Total feeding amount in a day
	Feeding cumulative	Cumulative calculation of feeding amount
Harvest (Operational)	Partial harvest cumulative	Cumulative calculation of partial harvest
	Partial harvest frequency	Frequency of partial harvest
Water (Environmental)	pH	pH measurement
	Temperature	Temperature measurement
	Salinity	Salinity measurement
	Dissolved oxygen	Dissolved oxygen measurement
	Alkalinity	Alkalinity measurement

2.2.2. Data Cleaning and Missing Data Handling

Missing data handling by feature category:

- Harvesting variables: Complete case removal (any incomplete harvest event removes entire pond/cycle).
- Water quality: Local 5-day median imputation for gaps $\leq$ 5 days.
- Daily feeding: Pond–cycle median substitution.
- Body weight: Linear interpolation within cycles.

This approach preserves causal interpretability while maintaining data integrity. Complete case removal for harvesting ensures biological validity and prevents artificial reconstruction of harvest events.

2.3. Water Quality Stability Assessment

Water quality parameters were assessed for environmental stability using the coefficient of variation (CV%), a scale-independent measure of relative variability enabling comparison across parameters with different units and magnitude ranges. CV% was calculated as CV (%) = (Standard Deviation/Mean) $\times$ 100. Stability thresholds were defined based on aquaculture industry standards: CV% < 5% indicates very stable conditions; 5–10% indicates stable conditions; 10–15% indicates moderate variability; and >15% indicates problematic instability. Five water quality parameters were analyzed: temperature (°C), pH (units), dissolved oxygen (mg/L), salinity (ppt), and alkalinity (mg/L). Descriptive statistics (mean, standard deviation, minimum, maximum, range) were calculated for each parameter across all observations from cleaned (eight production cycles across 12 ponds). All parameters were assessed for consistency within physiologically optimal ranges for *L. vannamei* aquaculture: temperature 26–32 °C, dissolved oxygen 4.0–8.0 mg/L, pH 7.0–9.0, salinity 20–30 ppt, and alkalinity 100–150 mg/L. This stability analysis provides critical context for interpreting machine learning feature importance results. In environments with variable environmental parameters, water quality is expected to emerge as a primary predictor of growth. However, in facilities where environmental stability is actively maintained, environmental factors function as production constraints rather than continuous predictors, and operational variables (partial harvesting, feeding management) would dominate predictions.

2.4. Feature Engineering and Preprocessing

2.4.1. Temporal Feature Engineering

Day of Cultivation (DoC) was defined as the number of days elapsed since post-larvae (PL) stocking. In the production dataset, DoC ranged from Day 30 to approximately Day 130, representing the measurement period from post-larvae transfer to production ponds (PL30) through final harvest.

Data collection began at Day 30 post-stocking (PL30), coinciding with the transfer of post-larvae from nursery facilities to production ponds. The nursery phase (Days 0–29, PL0–PL29) occurred in separate hatchery/nursery systems and was not included in the production analysis. Therefore, all DoC values in the modeling dataset represent days elapsed in the production environment, ranging from Day 30 to approximately Day 130.

DoC was used directly as a numerical feature without transformation, allowing the model to capture the temporal progression of growth throughout the production phase. No explicit seasonal features were engineered, as production cycles run continuously with minimal seasonal variation at the study facility in West Java, Indonesia (equatorial climate with consistent year-round conditions).

2.4.2. Cumulative Feature Calculation

Cumulative features were calculated sequentially within each pond–cycle combination:

- Cumulative Feeding = sum of daily feeding amounts from day 0 to day t;
- Cumulative Harvest Mass = sum of all partial harvest amounts from day 0 to day t;
- Partial Harvest Count = cumulative number of discrete harvest events from day 0 to day t.

These cumulative features capture integrated management intensity over the production cycle.

2.4.3. Feature Standardization

All features were z-score normalized (mean = 0, SD = 1) using training-set parameters and applied identically to the validation/test sets. This is essential for SVM and ANN, and less critical for tree-based models.

2.5. Model Development and Training

2.5.1. Cross-Validation Strategy

A 10-fold cross-validation approach was implemented (N_CV_SPLITS = 10) to ensure robust performance estimation. Data were organized by group (pond_id, cycle_id) to maintain spatial and temporal coherence within folds. For each fold:

- Training set: 9 folds (approximately 70% of data);
- Test set: 1 fold held out (approximately 10% of data).

2.5.2. Hyperparameter Grid Search Strategy

Hyperparameter optimization was conducted using Randomized Grid Search Cross-Validation (RandomizedSearchCV) with 80 random iterations (N_ITER_SEARCH = 80) and 10-fold cross-validation to identify optimal parameters for each model. Each algorithm has a different set of hyperparameters to be tuned over the iterations (Table 2).

2.5.3. Model Architectures

Seven ML approaches: Random Forest (tree ensemble), SVM (kernel-based, RBF), ANN (feedforward, ReLU, Huber loss), and LSTM (temporal, 72 enriched features, dropout). Ensembles: Voting (equal weights), Weighted (R^2-proportional), Stacking (Ridge meta-learner). All optimized via RandomizedSearchCV with 10-fold CV and early stopping.

Table 2. Hyperparameter list.

Algorithm	Hyperparameters	Grid
Random Forest	Number of trees	50, 100, 150, 200, 250
	Max depth	5, 10, 15, 20, 30
	Min. samples per leaf	1, 2, 4
	Min. samples per split	2, 5, 10
	Feature sampling	'sqrt', 'log2'
Support Vector Machine	Kernel	'linear', 'rbf', 'poly'
	C (Regularization)	0.1, 1, 10, 100, 1000
	Gamma (for rbf/poly)	'scale', 'auto', 0.001, 0.01
	Degree (for poly)	2, 3, 4
Artificial Neural Network	Hidden dimension	32, 48, 64, 96, 128
	Number of hidden layers	1, 2, 3
	Batch size	8, 16, 32
	Learning rate	0.0001, 0.0005, 0.001, 0.005
	Epochs (max)	80, 100, 150
	Early stopping patience	8, 10, 12
	Dropout	0.0, 0.2, 0.3, 0.4, 0.5
	Gradient clipping norm	1.0
Long Short-Term Memory	Hidden dimension	32, 64, 128
	Number of layers	1, 2, 3
	Batch size	8, 16, 32
	Learning rate	0.0005, 0.001, 0.002
	Epochs (max)	100, 150, 200
	Early stopping patience	8, 12, 16
	Dropout	0.0, 0.1, 0.2
	Gradient clipping norm	1.0 (conditional; only if num_layers > 1)
	Window size	Fixed at 14 days

2.5.4. Training Procedure

All models were trained on identical training sets for direct comparison. For neural network models (ANN and LSTM), early stopping was implemented, with patience values optimized via RandomizedSearchCV.

LSTM sequences were generated independently, with enriched temporal features within pond–cycle groups to respect production-cycle boundaries.

2.6. Performance Evaluation Metrics

Performance evaluated via MAE, RMSE (primary metric), R^2, and Relative Error (% of mean target), calculated across 10-fold CV (Table 3).

Table 3. Evaluation metrics and mathematical formulations: Model performance was evaluated using four complementary metrics that quantify different aspects of prediction quality. Mean Absolute Error (MAE) measures typical prediction error magnitude in grams and is robust to outliers. Root Mean Square Error (RMSE), the primary metric for model ranking, penalizes larger errors and is reported in grams. Coefficient of Determination (R^2, 0–1 scale) indicates the proportion of target variance explained by the model. Relative Error (percentage) enables comparison across aquaculture systems with different absolute growth scales. All metrics were calculated across a 10-fold cross-validation. Mathematical notation: n = sample size; y_i = observed mean body weight; $\hat{y}_i$ = predicted mean body weight; $\bar{y}$ = mean of observed values.

Metrics	Equation	Description
Mean Average Error (MAE)	$\frac{1}{n}\sum_{i=1}^{n}\lvert y_i - \hat{y}_i\rvert$	MAE represents typical prediction error magnitude and is robust to outliers.
Root Mean Square Error (RMSE)	$\sqrt{\frac{1}{n}\sum_{i=1}^{n}(y_i - \hat{y}_i)^2}$	RMSE emphasizes larger prediction errors and is reported in the same units as the target variable (grams).

Table 3. *Cont.*

Metrics	Equation	Description
Coefficient of Determination (R^2)	$\frac{\sum_{i=1}^{n}(\hat{y}_i-\overline{y})^2}{\sum_{i=1}^{n}(y_i-\overline{y})^2}$	R^2 indicates the proportion of target variance explained by the model (range: 0–1, where higher values indicate better fit).
Relative Error	$\frac{MAE}{\overline{y}} \times 100\%$	This metric expresses prediction error as a percentage of mean body weight, enabling comparison across systems with different absolute scales.

This metric expresses prediction error as a percentage of mean body weight, enabling comparison across systems with different absolute scales.

2.7. Statistical Analysis

Confidence Interval Calculation

Model stability and uncertainty were quantified using 95% confidence intervals (CIs) computed from cross-validation results. For each model, Root Mean Squared Error (RMSE) was calculated independently on each of the 10 test folds, producing 10 distinct RMSE values. These fold-level results were then used to estimate the mean RMSE and fold-level variability.

The 95% confidence interval was constructed using the t-distribution, which is appropriate for small sample sizes (10 folds). The calculation proceeded as follows: (1) the mean RMSE across all 10 folds was computed; (2) the sample standard deviation was calculated; (3) the standard error was determined by dividing the standard deviation by the square root of 10; and (4) the 95% CI was calculated by taking the mean RMSE plus or minus the critical t-value (for 9 degrees of freedom), multiplied by the standard error.

This approach directly quantifies fold-to-fold variability and reflects model stability across different pond and cycle groupings. The resulting confidence intervals indicate the range in which the true RMSE would fall with 95% confidence, given the observed distribution of performance across folds. Narrower confidence intervals indicate more stable predictions across folds, while wider intervals suggest greater sensitivity to data partitioning strategy. GroupKFold partitioning (respecting pond ecological boundaries and rearing cycles) ensures that confidence intervals reflect realistic uncertainty when predicting across new, ecologically distinct groups.

2.8. Feature Importance Analysis

2.8.1. Multi-Method Consensus Approach

Three independent feature importance methods established consensus:

1. LSTM Gradient Analysis: Mean absolute gradient of output vs. each feature;
2. Permutation importance: Mean RMSE increases when feature is shuffled (five repeats);
3. Consensus ranking: Averaged across Random Forest, SVM, and ANN.

2.8.2. Consensus Importance Calculation

Consensus feature importance was calculated as the mean importance score across all three models (Random Forest, SVM, and ANN). For each feature: consensus importance = (RF + SVM + ANN)/3. Features were ranked by consensus importance in descending order.

2.9. Pearson Correlation Analysis

Pearson correlation coefficients and corresponding *p*-values were computed for all features against the target (Mean Body Weight) across the entire dataset. Correlations with $p < 0.05$ were considered statistically significant at $\alpha = 0.05$. A correlation matrix heatmap was generated to visualize feature relationships and identify potential multicollinearity

among predictors. These correlations complemented model-based feature importance rankings, providing multiple perspectives on feature–target relationships.

2.10. SHAP (SHapley Additive exPlanations) Analysis

SHAP analysis on best model: TreeExplainer for tree models; KernelExplainer (100 background samples) for SVM/ANN. SHAP values calculated for 200 test samples across 14 features. Summary plots (beeswarm, bar chart) and dependence plots visualized feature contributions.

2.11. Convergence Validation

To validate that feature importance rankings were robust across independent methods, Spearman's rank correlation analysis was employed to compare rankings from different importance quantification approaches. Spearman's rank correlation (ρ) measures the agreement between two ranked lists, with values ranging from −1 (perfect negative correlation) to +1 (perfect positive correlation). Spearman ρ was calculated between consensus importance rankings and SHAP analysis rankings across all 14 features. Statistical significance was assessed at $\alpha = 0.05$.

3. Results

3.1. Data Characteristics and Preprocessing

The raw dataset initially comprised 15,683 records from 12 ponds over eight rearing cycles (2017–2022). To ensure data integrity for mechanistic interpretation, a complete-case analysis was applied to the harvesting variables, yielding a final dataset of 5479 records (34.94% retention). Within this dataset, water quality parameters demonstrated varying degrees of stability (Table 4). Temperature (CV 4.6%) and pH (CV 4.9%) showed tight control, while dissolved oxygen (9.8%), salinity (13.2%), and alkalinity (13.5%) exhibited moderate variability. Crucially, all parameters remained within species-appropriate ranges. Before modeling, all 14 core features were z-score normalized. For the LSTM architecture, the input space was enriched to 72 features using temporal transformations (delta, cumulative, and moving averages). A correlation matrix heatmap (Figure 1) revealed strong positive clustering among operational variables (feed, harvest) and mean body weight, while environmental variables showed weak or negative associations.

Table 4. Water quality parameter stability assessment.

Parameter	Mean	Std	CV
alkalinity	138.233	18.698	13.527
salinity	35.260	4.639	13.156
do	4.807	0.471	9.806
ph	8.190	0.405	4.941
temp	28.078	1.294	4.609

3.2. Model Performance and Stability

To ensure optimal generalization, hyperparameter tuning was conducted using RandomizedSearchCV across all base models (Table 5). In terms of predictive accuracy, distinct performance tiers emerged (Table 6). Among individual base models, the ANN achieved the lowest RMSE (1.534 g) and highest R^2 (0.950), outperforming the SVM and Random Forest baselines. However, the Weighted Ensemble demonstrated highly competitive performance ($R^2 = 0.948$, RMSE = 1.563 g) by assigning performance-proportional weights to the base learners (Table 7). Stability analysis via 10-fold GroupKFold cross-validation confirmed the robustness of these results. The ANN exhibited the tightest confidence bounds (0.708 g

width, CV% = 27.7%), indicating exceptional consistency across different pond–cycle groupings compared to the wider variance observed in RF and SVM models (Table 8).

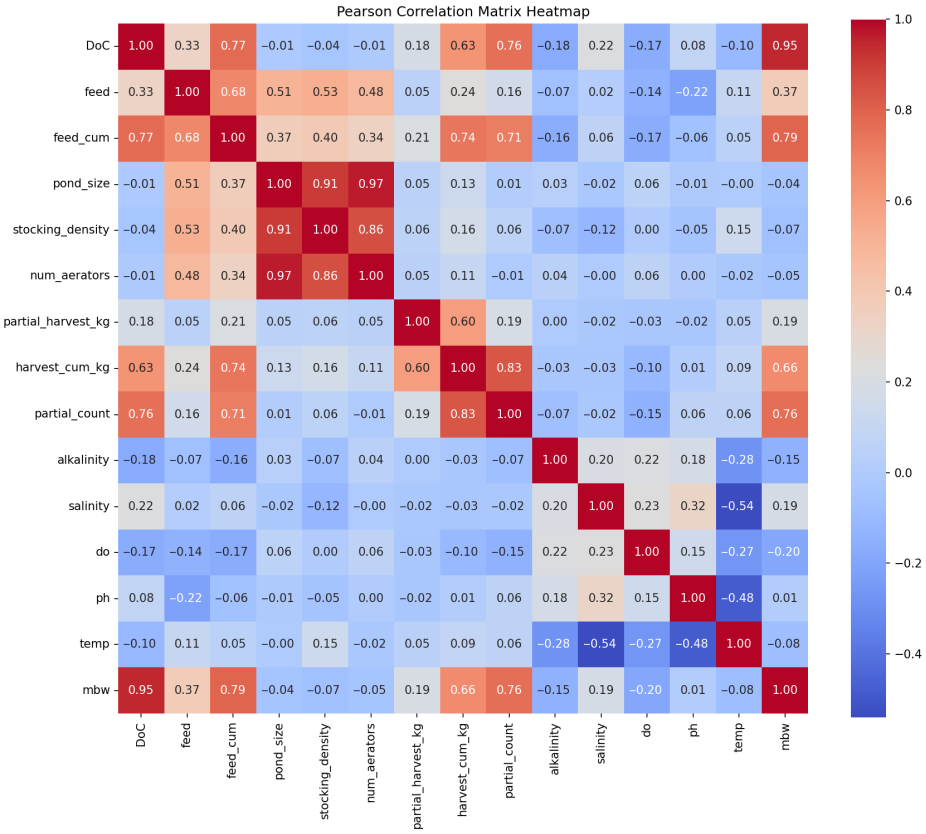


Figure 1. Correlation matrix heatmap showing all pairwise correlations between 14 features and mean body weight (mbw). Red indicates positive correlations, blue indicates negative correlations, and white indicates zero correlation. Features include DoC, feed, feed_cum, pond_size, stocking_density, num_aerators, partial_harvest_kg, harvest_cum_kg, partial_count, alkalinity, salinity, do, and ph. Harvesting-related variables (partial_harvest_kg, harvest_cum_kg, partial_count) show moderate to strong positive correlations with mbw (r = 0.19–0.76), while environmental variables show weak negative correlations (r = −0.08 to −0.20). DoC shows the strongest correlation with mbw (r = 0.95).

Table 5. Optimal hyperparameters identified by RandomizedSearchCV (80 random iterations, 10-fold cross-validation). The table presents the hyperparameter search grid for each algorithm, with final optimal values selected to minimize RMSE on validation folds. RF: Random Forest (150 trees, max depth 15, log2 feature sampling); SVM: Support Vector Machine (RBF kernel, C = 1000, gamma = 0.001; tested alternative poly kernel with degree 2); ANN: Artificial Neural Network (128 hidden units, batch size 32, learning rate 0.005, early stopping patience 12); LSTM: Long Short-Term Memory (32 hidden dimension, two layers, batch size: 8, learning rate: 0.005, early stopping patience: 16). Window size fixed at 14 days for LSTM temporal modeling. Early stopping parameters prevent overfitting by halting training if validation loss does not improve within the specified patience epochs.

Algorithm	Hyperparameters	Grid
Random Forest	Number of trees	150
	Max depth	15
	Min. samples per leaf	2
	Min. samples per split	5
	Feature sampling	‘log2’
Support Vector Machine	Kernel	‘rbf’
	C (Regularization)	1000
	Gamma (for rbf/poly)	0.001
	Degree (for poly)	2

Table 5. *Cont.*

Algorithm	Hyperparameters	Grid
Artificial Neural Network	Hidden dimension	128
	Number of hidden layers	1
	Batch size	32
	Learning rate	0.005
	Epochs (max)	150
	Early stopping patience	12
	Dropout	0.5
	Gradient clipping norm	1.0
Long Short-Term Memory	Hidden dimension	32
	Number of layers	2
	Batch size	8
	Learning rate	0.005
	Epochs (max)	150
	Early stopping patience	16
	Dropout	0.0
	Gradient clipping norm	1.0 (conditional; only if num_layers > 1)
	Window size	Fixed at 14 days

Fixed parameters: Window size: 14 days; Gradient clipping norm: 1.0 (when num_layers > 1); Loss function: Huber (delta = 1.0).

Table 6. Model performance metrics were evaluated via 10-fold cross-validation with 20 iterations per fold (200 total folds). RMSE (Root Mean Squared Error) measured prediction deviation in kilograms; MAE (Mean Absolute Error) measured mean absolute deviation; R^2 measured the proportion of variance explained (range 0–1, with 1 indicating perfect predictions). Relative Error (%) calculated as (RMSE/mean_target) × 100, representing prediction deviation as a percentage of the mean body weight. All metrics are reported as mean values across cross-validation folds. ANN achieved the lowest RMSE (1.534 g, 9.79% Relative Error), followed closely by Weighted Ensemble (1.563 g, 9.93% Relative Error, within 1.9% of ANN). Voting Ensemble also achieved a competitive performance (RMSE = 1.570 g). Stacking Ensemble underperformed other ensemble methods (RMSE = 1.834), suggesting that meta-learner combination did not improve upon simple averaging or performance-weighted averaging strategies for this dataset.

Model	RMSE (g)	MAE (g)	R-Square	Relative Error (%)	Training Time (s)
Random Forest	1.791	1.175	0.932	11.448	30.866
SVM	1.642	1.136	0.943	11.069	824.191
ANN	1.534	1.004	0.950	9.787	33,719.087
Voting Ensemble	1.570	1.023	0.947	9.968	0.233
Weighted Ensemble	1.563	1.019	0.948	9.928	0.130
Stacking Ensemble	1.834	1.201	0.928	11.708	0.524

Table 7. Weighted Ensemble model combination weights. Weights determined by inverse RMSE ranking across base models on the validation set. ANN achieved the lowest RMSE (1.534 g) and received the highest weight (0.358); SVM with intermediate RMSE (1.642 g) received the weight 0.335; Random Forest with the highest RMSE (1.791 g) received the lowest weight (0.307). Weights sum to approximately 1.0, enabling weighted averaging of base model predictions: Ensemble_prediction = 0.307 × RF_prediction + 0.335 × SVM_prediction + 0.358 × ANN_prediction. This weighting scheme allows the ensemble to adaptively combine base models with relative contributions proportional to their individual predictive performance.

Model	RMSE (g)	Weight
Random Forest	1.791	0.307
Support Vector Machine	1.642	0.335
Artificial Neural Network	1.534	0.358

(Weights sum to ~1.0).

3.3. Feature Importance and Interpretability

Consensus rankings identified temporal and operational variables as the primary drivers of shrimp growth. The Days of Culture (DoC) feature dominated the hierarchy,

accounting for 51.1% of total consensus importance (Table 9; Figure 2). Following DoC, operational variables such as feed_cum and stocking_density ranked second and third, respectively. Collectively, these top three features represented 81.0% of the total predictive power. Harvesting-related variables occupied the mid-range of importance, significantly outperforming infrastructure and environmental parameters. Cumulative harvest weight (rank 4) and partial harvest frequency (rank 5) contributed approximately 10.2% of the total consensus importance (Table 10). SHAP dependence analysis (Figure 3) further revealed that these operational features have a nonlinear, positive impact on biomass prediction, particularly in the later stages of the culture cycle.

Table 8. Cross-validation stability metrics for base models were evaluated via 10-fold GroupKFold cross-validation. RMSE_Mean represents the average RMSE across all 10 folds; RMSE_SD shows the standard deviation of RMSE values across folds; CV% (Coefficient of Variation) expresses this standard deviation as a percentage of the mean (CV% = 100 × SD/Mean), providing a scale-invariant measure of fold-to-fold variability; RMSE_95CI_Lower and RMSE_95CI_Upper are the lower and upper bounds of the 95% confidence interval calculated using the t-distribution with 9 degrees of freedom. Narrower confidence intervals indicate more consistent model performance across different pond/cycle groupings. ANN exhibited the narrowest confidence interval (0.708 g) and the lowest CV (27.7%), indicating stable predictions across folds. Random Forest and SVM showed wider confidence intervals (1.037 and 0.981 g, respectively) and higher CV values (38.0% and 40.2%), indicating greater sensitivity to fold composition.

Model	RMSE_Mean (g)	RMSE_SD	CV%	RMSE_95CI_Lower	RMSE_95CI_Upper
Random Forest	1.907	0.725	38.014	1.389	2.426
SVM	1.704	0.686	40.249	1.214	2.195
ANN	1.787	0.495	27.689	1.433	2.141

Table 9. Consensus feature importance rankings for shrimp mean body weight prediction, derived by averaging permutation importance scores across Random Forest, SVM, and Artificial Neural Network base models. The Consensus Score represents the mean importance value across all three algorithms. Features are ranked from highest (DoC, 4.213) to lowest importance (pH, 0.015) and categorized by type: Temporal (rearing cycle duration), Operational (farm management practices), Infrastructure (pond characteristics and equipment), and Environmental (water quality parameters). Harvesting-related variables (harvest_cum_kg, partial_count, partial_harvest_kg) ranked 4th, 5th, and 11th, respectively, among all features. DoC accounted for 51.1% of total consensus importance, with the top three features (DoC, feed_cum, stocking_density) collectively accounting for 81.0%.

Rank	Feature	Consensus Score	Category
1	DoC	4.213	Temporal
2	feed_cum	1.679	Operational
3	stocking_density	0.783	Operational
4	harvest_cum_kg	0.471	Operational
5	partial_count	0.342	Operational
6	pond_size	0.285	Infrastructure
7	num_aerators	0.140	Infrastructure
8	salinity	0.097	Environmental
9	feed	0.094	Operational
10	alkalinity	0.050	Environmental
11	partial_harvest_kg	0.032	Operational
12	do	0.020	Environmental
13	temp	0.019	Environmental
14	ph	0.015	Environmental

The Consensus Score represents the mean importance across all three algorithms (RF, SVM, ANN). Features are ranked in order of decreasing importance.

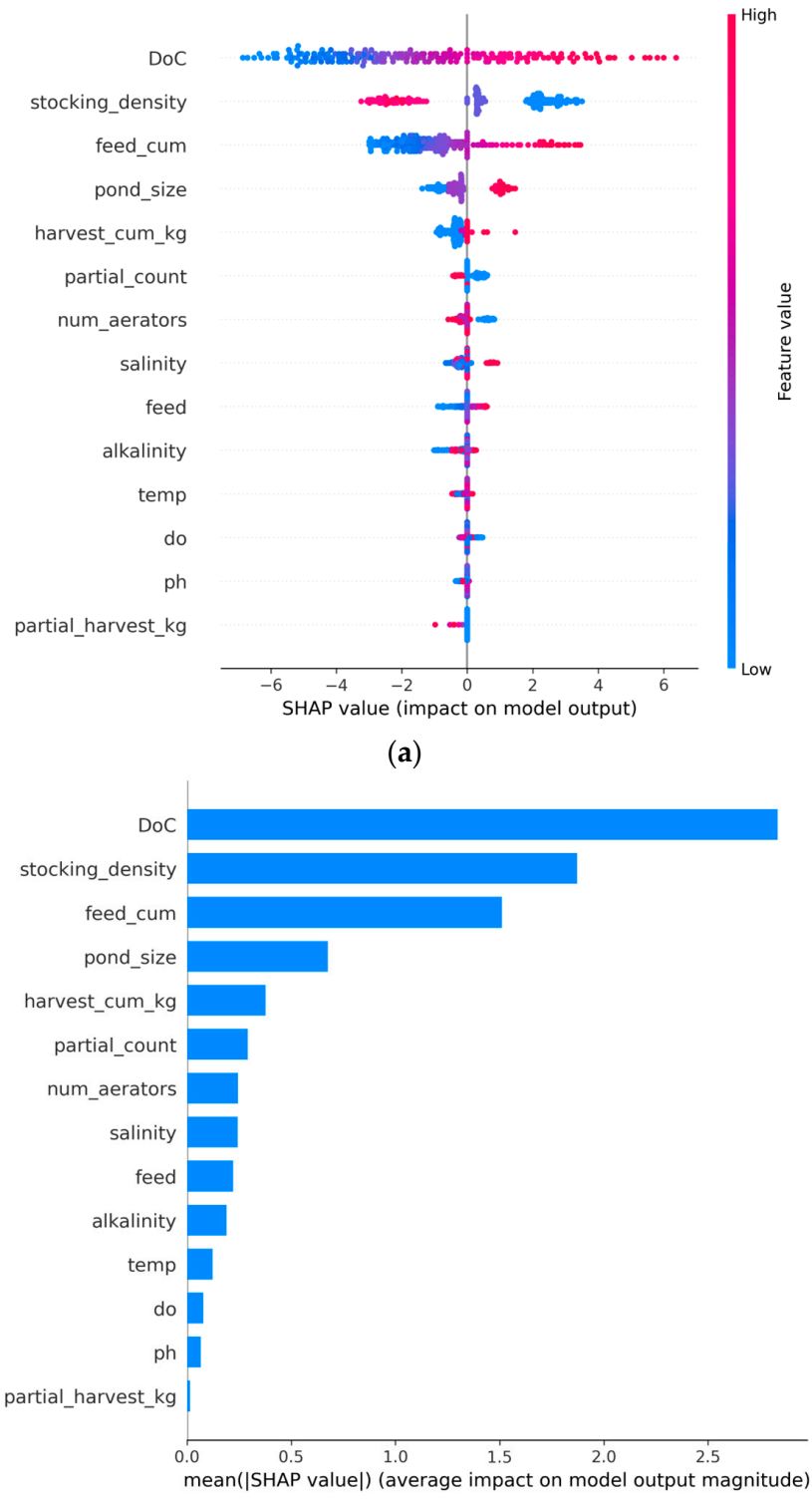


Figure 2. SHAP summary plots showing feature importance rankings. (**a**) A beeswarm plot displays individual sample SHAP values for each feature, ranked by mean absolute SHAP. Horizontal spread represents the range of SHAP values across samples; DoC shows the widest spread. Color gradient indicates feature values (blue = low values, red = high values). (**b**) A bar chart displays mean |SHAP| values, ranked from highest to lowest importance. DoC (2.833), stocking_density (1.871), and feed_cum (1.510) rank highest. Harvesting variables harvest_cum_kg and partial_count rank 5th and 6th, respectively; partial_harvest_kg ranks 14th.

Table 10. Feature importance by category with both total consensus scores and mean importance per feature. Mean Score represents the average consensus importance for features within each category (Total Score ÷ Number of Features). This normalization accounts for unequal category sizes: Temporal (1 feature, mean 4.213); Operational (6 features, mean 0.567, including three harvesting-related variables); Infrastructure (two features, mean 0.212); Environmental (five features, mean 0.040). The Operational category contained three harvesting-related variables (harvest_cum_kg: 0.471, partial_count: 0.342, partial_harvest_kg: 0.032), which collectively contributed 0.845 importance points to the operational category total of 3.400.

Rank	Category	Mean Score per Feature	Total Score	Number of Features
1	Temporal	4.213	4.213	1
2	Operational	0.567	3.400	6
3	Infrastructure	0.212	0.425	2
4	Environmental	0.040	0.201	5

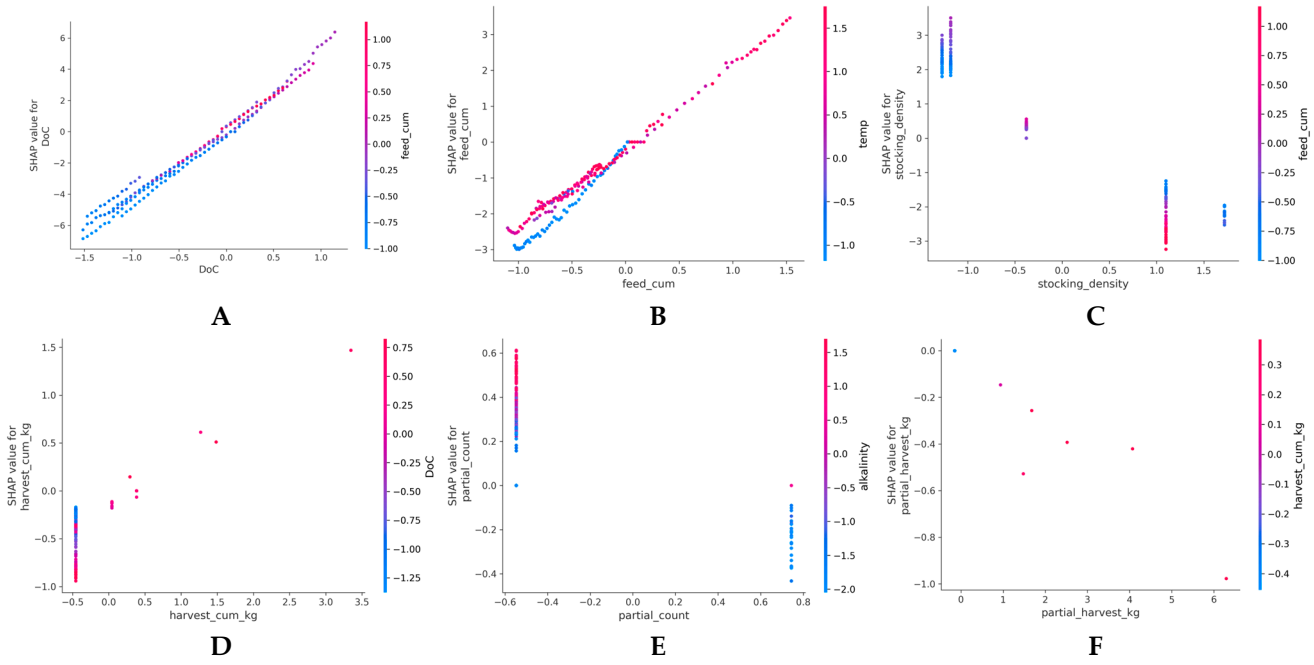


Figure 3. SHAP dependence plots for six key features showing normalized feature values (*X*-axis) versus SHAP values (*Y*-axis). (**A**) DoC demonstrates a linear positive relationship with SHAP values ranging from −6 to +7. (**B**) Feed_cum demonstrates a positive relationship with SHAP range ±3 and temperature interaction. (**C**) Stocking_density shows a negative relationship with SHAP values ranging from −3.5 to +3.0. (**D**) Harvest_cum_kg shows a positive nonlinear trend, with a SHAP range of ±1.5. (**E**) Partial_count shows a weak positive trend, with SHAP values ranging from ±0.6 and distinct clustering. (**F**) Partial_harvest_kg demonstrates sparse distribution with minimal SHAP variation (±1.0). Y-axis ranges differ by feature; larger ranges correspond to higher importance.

In contrast, environmental water quality variables showed negligible predictive influence. Dissolved oxygen, temperature, and pH occupied the lowest ranks (11th–13th), collectively representing less than 0.6% of total importance (Table 11). This lack of signal was corroborated by Pearson correlation analysis, which showed weak linear associations ($r < 0.1$) between water quality parameters and mean body weight (Table 12). To validate the robustness of these rankings, a convergence analysis was performed comparing consensus importance vs. SHAP rankings. The Spearman rank correlation was 0.947 ($p < 0.001$), indicating firm agreement between the independent methods and confirming that the feature hierarchy is a genuine property of the data rather than a model artifact.

Table 11. SHAP feature importance ranking for the best-performing ANN model based on mean absolute SHAP values across 200 test samples. Mean SHAP Contribution indicates the average signed SHAP value (negative values represent features that typically decrease predictions; positive values represent features that increase predictions). Std SHAP shows the standard deviation of SHAP values across samples. Three harvesting-related variables: harvest_cum_kg (rank 5), partial_count (rank 6), and partial_harvest_kg (rank 14). DoC ranks first (Mean |SHAP| = 2.833), followed by stocking_density (1.871) and feed_cum (1.510).

Rank	Feature	Mean |SHAP|	Mean SHAP Contribution	Std SHAP
1	DoC	2.833	−1.315	3.064
2	stocking_density	1.871	0.493	2.048
3	feed_cum	1.510	−0.911	1.482
4	pond_size	0.675	−0.035	0.766
5	harvest_cum_kg	0.376	−0.349	0.277
6	partial_count	0.292	0.235	0.249
7	num_aerators	0.244	0.024	0.337
8	salinity	0.243	−0.146	0.273
9	feed	0.221	−0.039	0.323
10	alkalinity	0.190	−0.164	0.244
11	temp	0.123	−0.120	0.146
12	do	0.077	0.019	0.138
13	ph	0.065	−0.064	0.089
14	partial_harvest_kg	0.014	−0.014	0.090

Table 12. Pearson correlation coefficients and statistical significance between features and mean body weight (mbw) across the entire dataset. Correlation coefficient (r) and two-tailed *p*-values are reported. Statistical significance at $\alpha = 0.05$ is indicated: *** $p < 0.001$, ** $p < 0.01$, ns = not significant. Of 14 features evaluated, 13 showed statistically significant correlations ($p < 0.05$), while pH was not significant ($p = 0.360$). Three harvesting-related variables: partial_count (r = 0.760, rank 3), harvest_cum_kg (r = 0.665, rank 4), and partial_harvest_kg (r = 0.194, rank 6). Positive correlations ranged from 0.012 to 0.940, while negative correlations ranged from −0.042 to −0.196.

Feature	r	*p*-Value	Significant
DoC	0.940	<0.001	***
feed_cum	0.7900	<0.001	***
partial_count	0.7600	<0.001	***
harvest_cum_kg	0.665	<0.001	***
feed	0.374	<0.001	***
partial_harvest_kg	0.194	<0.001	***
salinity	0.187	<0.001	***
ph	0.012	0.360	ns
pond_size	−0.042	0.002	**
num_aerators	−0.047	<0.001	***
stocking_density	−0.067	<0.001	***
temp	−0.079	<0.001	***
alkalinity	−0.145	<0.001	***
do	−0.196	<0.001	***

Pearson correlation coefficient (r) ranges from −1 to +1, with positive values indicating positive correlation and negative values indicating negative correlation. Significance levels: *** $p < 0.001$, ** $p < 0.01$, ns = not significant ($p > 0.05$).

4. Discussion

4.1. Operational Dominance vs. Environmental Constraints

This study fundamentally challenges the "environmental primacy" paradigm in aquaculture modeling. While the classical literature consistently identifies water quality (DO,

temperature, pH) as the dominant predictor of shrimp growth [11,12,35], our multi-method analysis (Consensus, SHAP, Pearson) reveals a complete inversion of this hierarchy in industrial settings. In this facility, operational variables—specifically density, feeding, and harvesting—outperformed environmental parameters by an order of magnitude (Figure 2).

This divergence is not a contradiction but a context-dependent paradox. In open or semi-intensive systems, environmental volatility is indeed the limiting factor [37,38]. However, in high-intensity industrial operations where water quality is engineered to remain stable (Table 4), these variables function as "hygienic constraints" rather than "growth drivers." Once the environment is stabilized, it ceases to predict variance, and the predictive signal shifts entirely to active management levers. This finding suggests that as the global industry modernizes toward super-intensive systems [2,26], the focus of predictive modeling must shift from monitoring "nature" to optimizing "operations."

4.2. The Role of Harvesting Strategies

The detection of bimodal clustering in harvesting strategies (Strategy A vs. B) offers a novel mechanistic insight that purely regression-based models miss. Strategy A (low-frequency harvest) represents a "volume-maximization" approach, where the model sees no unique signal from harvesting because the biomass is simply accumulating. Conversely, Strategy B (high-frequency harvest) represents a "value-maximization" approach. By selectively removing biomass, managers effectively "reset" the density constraints, allowing the remaining stock to accelerate growth.

Critically, the model assigns a substantial positive SHAP value to Strategy B, validating it as a growth-enhancing intervention rather than just a logistical event. This implies that partial harvesting is not merely a method for cash flow management but also a biological tool to extend the cohort's exponential growth phase artificially. The fact that our model could blindly "discover" these two distinct human management styles via SHAP values (Figure 3) confirms that machine learning can decode the latent logic of farm managers [39,40], offering a pathway to automate strategic decision-support.

4.3. Model Robustness and Validity

The reliability of these findings is anchored in the "triangulation" of three independent mathematical frameworks. It is rare for linear (Pearson), nonlinear (Random Forest/ANN), and game-theoretic (SHAP) methods to converge so precisely on the same feature hierarchy (Table 9 vs. Table 11). This convergence effectively rules out the possibility that the "operational dominance" finding is an artifact of a specific algorithm's bias [28,41]. Furthermore, the stability of the ANN model across cross-validation folds (Table 8) demonstrates that this signal is robust to temporal and spatial variations, making the "Operational Dominance" hypothesis highly generalizable within this class of industrial facilities.

4.4. Limitations and Future Directions

While this study establishes a clear "Operational Dominance" rule for high-tech farming, it should not be overgeneralized to low-tech systems. The suppression of environmental signals is a luxury of high capital investment; in standard earthen ponds across Southeast Asia, water quality is likely the key factor [37,42]. Therefore, the next frontier for this research is "Context-Aware AI." Future models should explicitly encode the farm's intensity level as a meta-feature, enabling the system to dynamically switch between "Environment-First" (for open ponds) and "Operation-First" (for industrial tanks) predictions. Validating this switch-over point through multi-site studies would complete the unified theory of shrimp growth prediction [43].

5. Conclusions

This study provides the first systematic evidence that, in industrial-scale aquaculture, the primary drivers of shrimp growth are operational decisions rather than environmental fluctuations. By applying explainable machine learning to 5 years of commercial data, we demonstrated that active management levers—specifically stocking density, feeding, and partial harvesting—outperform water-quality parameters by an order of magnitude. This contradicts the traditional "environmental primacy" view, suggesting that in modernized, controlled systems, water quality functions as a baseline constraint rather than a continuous predictor.

Methodologically, this work validates the utility of "Explainable AI" (XAI) in aquaculture. The discovery of two distinct harvesting strategies (volume-focused vs. value-focused) via SHAP clustering proves that machine learning can do more than predict mean body weight; it can decode the latent management logic of human operators.

For the industry, the implication is clear: investment in predictive analytics should prioritize the digitization of operational workflows (harvest logs, feed tables) over the endless multiplication of water quality sensors. As the sector moves toward precision farming, the next generation of growth models must treat the farm not just as a biological ecosystem, but as a managed industrial process in which human decisions are the strongest signal amid the noise.

Author Contributions: Conceptualization, M.A.A.A.M., F.F.N.A., G.G.I., and N.R.; methodology, M.A.A.A.M., F.F.N.A., G.G.I., and N.Y.; software, M.A.A.A.M. and G.G.I.; validation, M.A.A.A.M., Y.S., and N.Y.; formal analysis, M.A.A.A.M., G.G.I., and Y.S.; investigation, M.A.A.A.M., G.G.I., and N.R.; resources, G.G.I., N.R., and N.Y.; data curation, M.A.A.A.M., G.G.I., and N.R.; writing—original draft preparation, M.A.A.A.M.; writing—review and editing, M.A.A.A.M. and N.Y.; visualization, M.A.A.A.M.; supervision, Y.S. and N.Y.; project administration, M.A.A.A.M.; funding acquisition, M.A.A.A.M. and N.Y. All authors have read and agreed to the published version of the manuscript.

Funding: This research was funded by Japan Society for the Promotion of Science (JSPS) Grants-in-Aid for Scientific Research (called KAKENHI) Grant number 21H04738 and JST SPRING grant number JPMJSP2108.

Institutional Review Board Statement: This study utilized existing production data collected during routine aquaculture operations at the DW Bahari Aquaculture facility in Indonesia. No experimental animals were subjected to novel treatments, stress, or manipulation for this research. Data collection occurred as part of standard farm operations and monitoring practices. The research involved only retrospective data analysis of anonymized production records without intervention. Therefore, no specific animal ethics approval was required from an Institutional Review Board (IRB). However, the facility operator provided written consent for the use of data for research, and all data analysis was conducted in accordance with institutional data-handling guidelines.

Data Availability Statement: The data supporting this study's findings are available from the corresponding author upon reasonable request.

Acknowledgments: We gratefully acknowledge Dicky Wicaksono, owner of DW Bahari Aquaculture, for his invaluable cooperation and for providing comprehensive operational data spanning five years (2017–2022) from 12 intensive aquaculture ponds. This dataset was essential for conducting a systematic analysis of the predictive importance of harvesting variables for shrimp growth prediction. We also acknowledge the technical staff at DW Bahari Aquaculture for their assistance in data collection, validation, and contextualization.

Conflicts of Interest: Gun Gun Indrayana and Nina Rachminiwati are employed by the company PT. The other authors declare that the research was conducted in the absence of any commercial or financial relationships that could be construed as a potential conflict of interest.

Abbreviations

The following abbreviations are used in this manuscript:

ANN	Artificial Neural Network
CI	Confidence Interval
CV	Coefficient of Variation
CV%	Coefficient of Variation Percentage
DoC	Day of Cultivation
EMS	Early Mortality Syndrome
LSTM	Long Short-Term Memory
MAE	Mean Absolute Error
ML	Machine Learning
pH	Potential of Hydrogen
R^2	Coefficient of Determination
RF	Random Forest
RMSE	Root Mean Square Error
SHAP	SHapley Additive exPlanations
SPF	Specific Pathogen Free
SVM	Support Vector Machine
WSSV	White Spot Syndrome Virus

References

1. FAO. The State of World Fisheries and Aquaculture 2024. In *The State of World Fisheries and Aquaculture (SOFIA)*; FAO: Rome, Italy, 2024; ISBN 978-92-5-138763-4.
2. Shrimp Market Demand & Forecast 2025 to 2035. Available online: https://www.futuremarketinsights.com/reports/shrimp-market (accessed on 23 November 2025).
3. Naser, M.d.N.; Sarker, M.N.; Hosain, M.d.E. *Whiteleg shrimp Litopenaeus vannamei*: Current status, future prospects and opportunities for Bangladesh Aquaculture. *Bangladesh J. Zool.* **2022**, *50*, 143–184. [CrossRef]
4. Le, N.T.T.; Armstrong, C.W.; Brækkan, E.H.; Eide, A. Climatic Events and Disease Occurrence in Intensive *Litopenaeus vannamei* Shrimp Farming in the Mekong Area of Vietnam. *Aquaculture* **2024**, *587*, 740867. [CrossRef]
5. De Schryver, P.; Defoirdt, T.; Sorgeloos, P. Early Mortality Syndrome Outbreaks: A Microbial Management Issue in Shrimp Farming? *PLoS Pathog.* **2014**, *10*, e1003919. [CrossRef]
6. Gao, Y.; He, Z.; Vector, H.; Zhao, B.; Li, Z.; He, J.; Chu, Z. Effect of Stocking Density on Growth, Oxidative Stress and HSP 70 of Pacific White Shrimp *Litopenaeus vannamei*. *Turk. J. Fish. Aquat. Sci.* **2017**, *17*, 877–884. [CrossRef]
7. Strebel, L.M.; Nguyen, K.; Araujo, A.; Corby, T.; Rhodes, M.; Beck, B.H.; Roy, L.A.; Davis, D.A. On Demand Feeding and the Response of *Pacific white shrimp* (*Litopenaeus vannamei*) to Varying Dietary Protein Levels in Semi-Intensive Pond Production. *Aquaculture* **2023**, *574*, 739698. [CrossRef]
8. Dorgham, H.M.; Badran, M.F.; El-Dakar, A.Y. Evaluation of Smart Fish Feeding System Using Artifi-cial Intelligence and Internet of Things under Desert Regions. *Mediterr. Aquac. J.* **2025**, *12*, 40–51. [CrossRef]
9. Arfiati, D.; Buwono, N.R.; Musa, M.; Prihanto, A.A.; Maftuch, M.; Mahmudi, M.; Dailami, M.; Amin, A.A.; Rangkuti, R.F.A.; Lusiana, E.D. A Comparative Analysis of Machine Learning Regression Models of *Whiteleg shrimp* Growth Reared in Eco-Green Aquaculture System. *Ecol. Eng. Environ. Technol.* **2025**, *26*, 146–154. [CrossRef]
10. Chen, F.; Sun, M.; Du, Y.; Xu, J.; Zhou, L.; Qiu, T.; Sun, J. Intelligent Feeding Technique Based on Predicting Shrimp Growth in Recirculating Aquaculture System. *Aquac. Res.* **2022**, *53*, 4401–4413. [CrossRef]
11. Rajonhson, D.M.; Angthong, P.; Thepsuwan, T.; Sutheeworapong, S.; Satanwat, P.; Tapaneeyaworawong, P.; Powtongsook, S.; Kruasuwan, W.; Jenjaroenpun, P.; Wongsurawat, T.; et al. Integrating Short- and Full-Length 16S rRNA Gene Sequencing to Elucidate Microbiome Profiles in Pacific *White shrimp* (*Litopenaeus vannamei*) Ponds. *Microbiol. Spectr.* **2024**, *12*, e00965-24. [CrossRef]
12. Ariadi, H.; Fadjar, M.; Mahmudi, M. The Relationships between Water Quality Parameters and the Growth Rate of *White shrimp* (*Litopenaeus vannamei*) in Intensive Ponds. *Aquac. Aquar. Conserv. Legis.* **2019**, *12*, 2103–2116.
13. Ashraf Rather, M.; Ahmad, I.; Shah, A.; Ahmad Hajam, Y.; Amin, A.; Khursheed, S.; Ahmad, I.; Rasool, S. Exploring Opportunities of Artificial Intelligence in Aquaculture to Meet Increasing Food Demand. *Food Chem. X* **2024**, *22*, 101309. [CrossRef]

14. Krivoguz, D.; Ioshpa, A.; Chernyi, S.; Zhilenkov, A.; Kustov, A.; Moiseev, I.; Serebryakov, M.; Kaynova, T.; Vorontsov, D.; Gritsenko, K. Real-Time Epizootic Monitoring with Inception Deep Neural Network for Maritime Applications. *Trans. Marit. Sci.* **2025**, *14*, e13051. [CrossRef]
15. Islam, S.I.; Ahammad, F.; Mohammed, H. Cutting-edge Technologies for Detecting and Controlling Fish Diseases: Current Status, Outlook, and Challenges. *J. World Aquac. Soc.* **2024**, *55*, e13051. [CrossRef]
16. Yu, R.; Leung, P. Optimal Partial Harvesting Schedule for Aquaculture Operations. *Mar. Resour. Econ.* **2006**, *21*, 301–315. [CrossRef]
17. Shi, Y.; Yan, L.; Zhang, S.; Tang, F.; Yang, S.; Fan, W.; Han, H.; Dai, Y. Revealing the Effects of Environmental and Spatio-Temporal Variables on Changes in *Japanese sardine* (*Sardinops melanostictus*) High Abundance Fishing Grounds Based on Interpretable Machine Learning Approach. *Front. Mar. Sci.* **2025**, *11*, 1503292. [CrossRef]
18. Xu, H.; Wu, Z.; He, H.; Chen, R.; Wu, X. Quantitative Analysis of the Uncertainty of Drought Process Simulation Based on Atmospheric–Hydrological Coupling in Different Climate Zones. *Water* **2023**, *15*, 3286. [CrossRef]
19. Karataş, B.; Çakmakçı, C.; Yücel, E.S.; Demir, M.; Şen, F. Using Different Machine-Learning Algorithms to Predict Dissolved Oxygen Concentration in *Rainbow trout* Farms. *Turk. J. Fish. Aquat. Sci.* **2025**, *26*, TRJFAS27622. [CrossRef]
20. Yang, X.; Zhang, S.; Liu, J.; Gao, Q.; Dong, S.; Zhou, C. Deep Learning for Smart Fish Farming: Applications, Opportunities and Challenges. *Rev. Aquac.* **2021**, *13*, 66–90. [CrossRef]
21. Hu, J.; Yin, J.; Yang, C.; Zhou, Y.; Li, C. Intelligent Forecasting Model for Aquatic Production Based on Artificial Neural Network. *Front. Mar. Sci.* **2025**, *12*, 1556294. [CrossRef]
22. Nayan, A.-A.; Saha, J.; Mozumder, A.N.; Mahmud, K.R.; Al Azad, A.K.; Kibria, M.G. A Machine Learning Approach for Early Detection of Fish Diseases by Analyzing Water Quality. *Trends Sci.* **2021**, *18*, 351. [CrossRef]
23. Eder, M.S.; Ampolitod, K.C.; Bolao, N.H.; Pajal, R.J.A.; Racho, E.M.D. SHRIMPAI: A Mobile Application for the Early Detection of White Spot Syndrome Virus in Shrimp Using Convolutional Neural Network. *Mindanao J. Sci. Technol.* **2024**, *22*, 196–220. [CrossRef]
24. Ramachandran, L.; Mohan, V.; Senthilkumar, S.; Ganesh, J. Early Detection and Identification of White Spot Syndrome in Shrimp Using an Improved Deep Convolutional Neural Network. *J. Intell. Fuzzy Syst.* **2023**, *45*, 6429–6440. [CrossRef]
25. Ragab, S.; Hoseinifar, S.H.; Van Doan, H.; Rossi, W.; Davies, S.; Ashour, M.; El-Haroun, E. Overview of Aquaculture Artificial Intelligence (AAI) Applications: Enhance Sustainability and Productivity, Reduce Labor Costs, and Increase the Quality of Aquatic Products. *Ann. Anim. Sci.* **2025**, *25*, 441–453. [CrossRef]
26. Akram, W.; Din, M.U.; Soud, L.S.; Hussain, I. A Review of Generative AI in Aquaculture: Foundations, Applications, and Future Directions for Smart and Sustainable Farming. *arXiv* **2025**, arXiv:2507.11974. [CrossRef]
27. Salih, A.; Raisi-Estabragh, Z.; Galazzo, I.B.; Radeva, P.; Petersen, S.E.; Menegaz, G.; Lekadir, K. A Perspective on Explainable Artificial Intelligence Methods: SHAP and LIME. *Adv. Intell. Syst.* **2023**, *7*, 2400304. [CrossRef]
28. Lundberg, S.; Lee, S.-I. A Unified Approach to Interpreting Model Predictions. *arXiv* **2017**, arXiv:1705.07874. [CrossRef]
29. Mohan, R.N.V.J.; Rayanoothala, P.S.; Sree, R.P. Next-Gen Agriculture: Integrating AI and XAI for Precision Crop Yield Predictions. *Front. Plant Sci.* **2025**, *15*, 1451607. [CrossRef] [PubMed]
30. Xu, S.-H.; Wang, S. An Intelligent Identification for Pest and Disease Detection in *Wheat leaf* Based on Environmental Data Using Multimodal Data Fusion. *Front. Plant Sci.* **2025**, *16*, 1608515. [CrossRef] [PubMed]
31. Arrighi, L.; de Moraes, I.A.; Zullich, M.; Simonato, M.; Barbin, D.F.; Junior, S.B. Explainable Artificial Intelligence Techniques for Interpretation of Food Datasets: A Review. *arXiv* **2025**, arXiv:2504.10527. [CrossRef]
32. Alirezazadeh, P.; Rahimi-Ajdadi, F.; Abbaspour-Gilandeh, Y.; Landwehr, N.; Tavakoli, H. Improved Digital Image-Based Assessment of Soil Aggregate Size by Applying Convolutional Neural Networks. *Comput. Electron. Agric.* **2021**, *191*, 106499. [CrossRef]
33. Jana, R.; Dixit, S.; Sharma, M.; Kumar, R. An Explainable AI Based Approach for Monitoring Animal Health. *arXiv* **2025**, arXiv:2508.10210. [CrossRef]
34. Abdel-Wareth, A.A.A.; Ahmed, A.A.; Salahuddin, M.; Lohakare, J. Application of Artificial Intelligence in Rabbit Husbandry: From Reproductive Monitoring to Precision Farming. *Front. Vet. Sci.* **2025**, *12*, 1679630. [CrossRef] [PubMed]
35. Siddique, M.A.B.; Mahalder, B.; Haque, M.M.; Ahammad, A.K.S. Impact of Climatic and Water Quality Parameters on *Tilapia* (*Oreochromis niloticus*) Broodfish Growth: Integrating ARIMA and ARIMAX for Precise Modeling and Forecasting. *PLoS ONE* **2025**, *20*, e0313846. [CrossRef]
36. Yang, H.; Liu, S. A Prediction Model of Aquaculture Water Quality Based on Multiscale Decomposition. *Math. Biosci. Eng.* **2021**, *18*, 7561–7579. [CrossRef]
37. Ray, A.J.; Dillon, K.S.; Lotz, J.M. Water Quality Dynamics and Shrimp (*Litopenaeus vannamei*) Production in Intensive, Mesohaline Culture Systems with Two Levels of Biofloc Management. *Aquac. Eng.* **2011**, *45*, 127–136. [CrossRef]
38. Boyd, C.E.; Tucker, C.S. *Pond Aquaculture Water Quality Management*; Springer: Boston, MA, USA, 2012.

39. Estrada-Pérez, A.; Ruiz-Velazco, J.M.J.; Hernández-Llamas, A.; Zavala-Leal, I.; Martínez-Cárdenas, L. Deterministic and Stochastic Models for Analysis of Partial Harvesting Strategies and Improvement of Intensive Commercial Production of *Whiteleg shrimp* (*Litopenaeus vannamei*). *Aquac. Eng.* **2016**, *70*, 56–62. [CrossRef]
40. González-Romero, M.A.; Ruiz-Velazco, J.M.J.; Estrada-Pérez, M.; Nieto-Navarro, J.T.; Zavala-Leal, I.; Hernandez-Llamas, A. Assessing Uncertainty of Semi-Intensive Production of *Whiteleg shrimp* (*Litopenaeus vannamei*) Using Partial Harvesting Programs. *Aquac. Res.* **2018**, *49*, 953–962. [CrossRef]
41. Molnar, C. *Interpretable Machine Learning*; Christoph Molnar: Morrisville, NC, USA, 2020.
42. Boyd, C.E. *Water Quality: An Introduction*; Springer International Publishing: Cham, Switzerland, 2015; ISBN 978-3-319-17445-7.
43. Zhao, S.; Zhang, S.; Liu, J.; Wang, H.; Zhu, J.; Li, D.; Zhao, R. Application of Machine Learning in Intelligent Fish Aquaculture: A Review. *Aquaculture* **2021**, *540*, 736724. [CrossRef]

Disclaimer/Publisher's Note: The statements, opinions and data contained in all publications are solely those of the individual author(s) and contributor(s) and not of MDPI and/or the editor(s). MDPI and/or the editor(s) disclaim responsibility for any injury to people or property resulting from any ideas, methods, instructions or products referred to in the content.